Published in final edited form as:
Glia. 2011 April ; 59(4): 577–589. doi:10.1002/glia.21126.

Expression of LPP3 in Bergmann glia is required for proper cerebellar sphingosine-1-phosphate metabolism/signaling and development

Alejandro López-Juárez[¥], **Sara Morales-Lázaro**[¥], **Roberto Sánchez-Sánchez**[¥], **Manjula Sunkara**[∫], **Hilda Lomelí**[§], **Iván Velasco**[¥], **Andrew J. Morris**[∫], and **Diana Escalante-Alcalde**[¥,*]

[¥]Instituto de Fisiología Celular, División de Neurociencias, Universidad Nacional Autónoma de México

[∫]University of Kentucky, College of Medicine, Lexington KY

[§]Instituto de Biotecnología, Universidad Nacional Autónoma de México

Abstract

Bioactive lipids serve as intracellular and extracellular mediators in cell signaling in normal and pathological conditions. Here we describe that an important regulator of some of these lipids, the lipid phosphate phosphatase-3 (LPP3), is abundantly expressed in specific plasma membrane domains of Bergmann glia (BG), a specialized type of astrocyte with key roles in cerebellum development and physiology. Mice selectively lacking expression of LPP3/*Ppap2b* in the nervous system are viable and fertile but exhibit defects in postnatal cerebellum development and modifications in the cytoarchitecture and arrangement of BG with a mild non-progressive motor coordination defect. Lipid and gene profiling studies in combination with pharmacological treatments suggest that most of these effects are associated with alterations in sphingosine-1-phosphate (S1P) metabolism and signaling. Altogether our data indicate that LPP3 participates in several aspects of neuron-glia communication required for proper cerebellum development.

Keywords

cerebellum; lipid phosphate phosphatase; S1P; $S1P_1$; astrocytes

INTRODUCTION

Lysophospholipids (LPs) such as lysophosphatic acid (LPA) and S1P play important roles in central nervous system (CNS) development, physiology and disease. The biosynthetic machinery and receptors responsible for LPs production and signaling are broadly distributed in the embryonic and adult brain with strong expression in neurogenic areas. *In vitro* studies have shown that LPA and S1P alter several cellular responses in neurons and glia (Brindley and Bräuer 2009; Milstien et al. 2007). Both have potent neurite retracting activity in postmitotic neurons and neuronal cell lines, through the activation of Rho signaling (Fukushima et al. 2002; Postma et al. 1996; Sato et al. 1997) and serve as regulators of neuroblast morphology and migration (Fukushima et al. 2000; Kimura et al. 2007). Additionally, LPA and S1P modulate intracellular Ca^{2+} in neurons and glia (Giussani et al. 2007; Holtsberg et al. 1997), promote astrocytic proliferation (Bassi et al. 2006; Shano

[*]Corresponding author: Diana Escalante-Alcalde, Instituto de Fisiología Celular-UNAM, Circuito Exterior s/n Ciudad Universitaria, México D. F. 04510, Coyoacán, Tel. (5255) 5622-5660, Fax (5255) 5622-5607, descalante@ifc.unam.mx.

et al. 2008) and modulate neuronal excitability (Sim-Selley et al. 2009; Trimbuch et al. 2009).

In ex vivo experiments, activation of LPA receptors induces folding and widening of the embryonic cerebral cortex, due to decreased cell death and increased terminal mitosis (Kingsbury et al. 2003). In contrast, a sub-line of *Lpar1* knockout mice, shows abnormal cortical development and increased cell death (Estivill-Torrus et al. 2008). Mice lacking receptor $S1P_1$ show increased cell death and reduced proliferation in the forebrain and die past mid-gestation due to defective vascular maturation (Mizugishi et al. 2005). The targeted inactivation of *S1pr2* yielded viable animals with no apparent anatomical or physiological defects, although they show sporadic seizures and increased excitability of neocortical pyramidal neurons (MacLennan et al. 2001). These observations show that LPA- and S1P-receptor mediated signaling play fundamental roles in CNS development and in modulating neuron excitability. In addition, abnormal S1P and LPA signaling participate in the etiology of several neuropathological conditions (Dennis et al. 2005; Nixon 2009).

Determining the specific *in vivo* function of these LPs has been precluded in part due to the elevated number of existing receptors and the apparent redundancy between them. However, studies of the enzymes that synthesize or metabolize these lipids strongly supports their role in development, normal physiology and disease. That is the case of autotaxin (Dennis et al. 2005; van Meeteren et al. 2006), sphingosine kinases (Mizugishi et al. 2005), sphingosine-1-phosphate lyase (Fyrst and Saba 2008), lipid phosphate phosphatases (LPPs) (Escalante-Alcalde et al. 2003) and LPP-related proteins (Trimbuch et al. 2009).

LPPs are a family of integral membrane enzymes with a wide spectrum lipid phosphate phosphohydrolase activity. Mammalian LPPs hydrolyze phosphatidic acid and ceramide-1-P besides LPA and S1P, originating diacylglycerol, ceramide, monoacylglycerol and sphingosine, respectively (Brindley et al. 2009). For this reason LPPs are considered regulators of the biological responses mediated by these lipids. Among the three LPPs described in mice, LPP3/*Ppap2b* is the only one which is essential for embryo development (Escalante-Alcalde et al. 2003), suggesting particular and non-redundant functions for this enzyme.

The role of LPPs in the development and function of the CNS has not been explored. In this paper we show that neural deficiency of LPP3 produces a mild motor coordination defect and abnormalities in cerebellar foliation, the latter related to alterations in the morphology, distribution and density of BG cells during cerebellum development. Remarkably, lack of LPP3 also leads to increased S1P concentration and down-regulation of $S1P_1$ receptor in the cerebellum indicating that this enzyme is a key modulator of S1P signaling in this region. Pharmacological treatment with a $S1P_1$ functional antagonist partially mimics the alterations found in BG strongly suggesting that the observed cerebellar alterations are associated to abnormal $S1P/S1P_1$ metabolism and signaling.

MATERIALS AND METHODS

Mouse strains and generation of neural-specific LPP3-knockout mice

For gene expression analysis, the $Ppap2b^{tm2Stw}$ allele ($Ppap2b^{lacZ}$), expressing β-galactosidase (β-gal) as a reporter was used (Escalante-Alcalde et al. 2009). For neural inactivation of LPP3, homozygous or heterozygous conditional $Ppap2b^{tm3Stw}$ ($Ppap2b^{flox}$) females were crossed with *Tg(Nes-cre)1Kln;* $Ppap2b^{tm3Stw/+}$ or $Ppap2b^{tm3Stw/tm3Stw}$ males and their progeny were genotyped by PCR from genomic DNA of neural and non-neural tissues as previously described (Escalante-Alcalde et al. 2007).

Motor coordination tests

Gross motor coordination defects were assessed on a Rotarod using two fixed rotation speeds in 1 month-old animals. After two training sessions, animals were placed on the Rotarod for 240 seconds, or until they fell off (latency to fall). Regardless of completion or fall, each animal was allowed to rest for 2 minutes between each trial. Each testing session consisted of 10 trials. Animals were tested at 20 rpm and 30 rpm on consecutive days and data expressed as the mean ± s.e.m. To assay for fine motor coordination defects, animals of one month of age were subjected to the beam-walking test. Performance was determined by measuring the time (up to 240 seconds) that mice were able to stay on round beams of two different diameters (5 and 7 mm). Another parameter evaluated was their behavior while walking on the beam. These tests were repeated in one year-old animals.

Immunohistochemistry, immunofluorescence, TUNEL and confocal microscopy

Perfused brains were fixed ON in 4% paraformaldehyde and 30 μm sagittal slices were obtained in a vibratome (Leica Microsystems). Floating sections were permeabilized and blocked with 1% Blocking Reagent (Roche) in PBS-Tween 0.3% for 2 hours. Antibodies (Abs) were diluted in blocking solution and incubated ON at 4°C: Rabbit anti-LPP3 (1:200), rabbit anti-Calbindin (1:100, Millipore), mouse anti-Parvalbumin (1:1000, Sigma), rabbit anti-BLBP (1:200), rabbit anti-GFAP (1:1000), rabbit anti-pHistone-H3 (1:100, Cell Signaling). For some Abs, sections were mounted on slides and treated with Antigen Unmasking Solution (Vector) followed by immunoperoxidase/nickel (Vectastain kit, Vector) or immunofluorescence: mouse anti-PCNA (1:100, Vector); guinea pig anti-Glast (1:1000); rabbit anti-p27 (1:100, Santa Cruz); mouse anti-S100B (1:100, Millipore); rabbit anti-EDG1 (1:100). Appropriate secondary Abs coupled to Alexa-488, Alexa-594 (Invitrogen), Texas Red or Cy5 (Jackson) were used for double and triple immunofluorescence. For TUNEL, sections were mounted and treated following provider's instructions (Boheringer, Germany). Sections were examined under a FV1000 confocal microscope (Olympus). Dual- or triple-color images were acquired using sequential acquisition to avoid cross-excitation. For co-localization experiments or high-resolution data, images were acquired with confocal aperture between 80–100 nm.

Cell counting

Confocal images acquired with equivalent conditions and in corresponding cerebellar regions were analyzed in sagittal sections at the mid vermis. Purkinje (PC) and BG cell somas found in the area corresponding to 300 μm of Purkinje cell layer (PCL) (defined as area unit) were counted. Identification of PC and BG was by parvalbumin or calbindin and BLBP immunoreactivity, respectively. For interneurons and ectopic BG cell somas in the molecular layer (ML), parvalbumin- and BLBP-positive cell somas were counted in the area of ML between 300 μm of PCL and the pia (defined as area unit). Phospho-Histone-H3 and TUNEL positive cells found in the external granule layer (EGL), PCL and ML (if present) were counted per lobe or folia taking as boundaries the deepest part of the sulcus between folias. The total number of positive cells/layer/cerebellum was counted. Number of positive cells in conditional neural specific knockouts, were expressed as the percentage of control littermates (100%).

Quantification of glycero- and sphingo-phospholipids by high-pressure liquid chromatography and tandem mass spectrometry (LC-MS /MS)

Lipids from perfused cerebellar tissue (around 20 mg wet weight) were extracted using acidified organic solvents with 50 pmol C17 LPA added as a recovery standard. Samples were evaporated to dryness, and redissolved in 4:1 MeOH; $CHCl_3$ for determination of phospholipid phosphorous and analysis by HPLC electrospray ionization tandem mass

spectrometry using selective reaction monitoring mode assays and methods that have been described in detail elsewhere to measure PA, LPA and S1P (Albers et al. 2010; Mathews et al. 2010; Miriyala et al. 2010; Su et al. 2009). Data were corrected for recovery of the C17 LPA internal standard and lipid species were quantitated by reference to calibration curves generated using synthetic standards (Avanti Polar Lipids) that were independently quantitated by lipid phosphorous determination. The data shown are means of triplicate measurements made with independent samples.

Pharmacological treatment with FTY720 in vitro and in vivo

For cerebellar organotypic slice cultures, anesthetized wildtype (ICR strain) or genetically modified mice at P7 were perfused with artificial cerebral spinal fluid, the cerebellum aseptically removed and cut into 300 μm sagittal sections. Slices were then transferred to Millicell CM culture inserts (Millipore) in 35 mm culture dishes containing 1 ml of medium (DMEM-F12 50%, horse serum 25%, HBSS 25%, glutamine 1 mM, KCl 25 mM, glucose 6 mg/ml, and antibiotics) and maintained for 48 hrs at 37° and 5% CO_2. Treatments (vehicle or FTY720 100 nM, Caiman Chemical) were added at the start of the culture. Slices were fixed ON with methanol-DMSO (4:1) and stained in whole mount against BLBP by immunofluorescence. Each experimental group was visualized using the same optical parameters under the confocal microscope. For *in vivo* treatments, FTY720 (0.3 μg/g of body weight) or vehicle was administered by intraperitoneal injection (i.p.) to mice from P3 to P14 and immunofluorescence or immunohistochemistry was performed as described earlier.

RESULTS

LPP3 is highly abundant in specific plasma membrane domains of Bergmann glia cells

LPP3 expression was initially analyzed in whole brain using a previously described *Ppap2b*-reporter allele (Escalante-Alcalde et al. 2009). In adult mice, β-gal was most strongly detected in the cerebellar cortex, followed by the olfactory bulb, the rostral migratory stream and the ventricular system. A less conspicuous expression was found in the hypothalamus (Fig. 1A). Within the cerebellum, β-gal was restricted to the ML and PCL (Fig. 1B), being the somata of the BG the region with strongest reporter activity. Mature BG cells are unipolar astrocytes located around the somas of PC (around 8 BG/per PC). Each BG cell gives rise to several intermediate filament-rich radial processes that traverse the ML and end at the pial surface. Each radial process is decorated with small secondary processes and a complex system of small lateral appendages rich in neurotransmitter transporters (i.e. Glast), which are in close interaction with synapses (Grosche et al. 2002; Yamada and Watanabe 2002) participating in removal of neurotransmitters released during synaptic activity (Bordey and Sontheimer 2003; Huang and Bordey 2004). During postnatal cerebellum development BG cells participate in the radial migration of external granule cells (EGC) as they use BG radial processes as guidelines to reach the internal granule layer (IGL) (Rakic 1971) and assist the morphogenesis of the PC dendritic tree (Yamada et al. 2000). Furthermore, it has been recently described that adult BG cells exhibit stem-cell like properties (Alcock and Sottile 2009).

The expression pattern revealed with our *Ppap2b* reporter allele resembles the mRNA expression pattern of the rat homolog (Suzuki et al. 1999) however no studies describing LPP3 protein distribution in BG cells exist. To examine the subcellular localization of LPP3 in adult BG cells we performed double or triple immunofluorescence using Abs against LPP3 and for markers of BG (Glast, S100B) and PC/interneurons (Parvalbumin) (Fig. 1C–Q). LPP3 was expressed in the entire ML, with a similar pattern to that of Glast (Fig. 1C–F, I–K), which is expressed in the plasma membrane-domains of BG that ensheath the dentritic

tree of PC (Yamada et al. 2000). Confocal analysis showed that LPP3 co-localized with Glast but was absent in PC and interneurons (Fig. 1G, H, O). Furthermore, LPP3 expression in BG cells also co-localized with S100B-positive lateral branches but was absent on radial processes (Fig. 1L–N), except for some near the pial surface (Fig. 1P). These results show that LPP3 in BG cells is restricted to the plasma membrane domains that ensheath the PC dendritic trees and synapses, and suggest that it participates in some aspects of the neuron-glia communication in the adult cerebellar cortex.

BG precursors are generated in the ventricular zone (VZ) of the cerebellar primordium around embryonic day 13 (E13) (Miyake et al. 1995) and migrate towards the cortex due to shortening of their radial processes adhered to the pial surface through their end feet (Yuasa 1996). Around the perinatal stage, the Glast-positive somas of BG organize into the PCL in a rostral-caudal fashion, while their radial processes cross the EGL and their end feet form the glia limitans at the pial surface (Yamada et al. 2000). BG shafts provide scaffolding during external granule cell radial migration, while the development of their fine lateral reticular processes accompanies the ensheathment of the developing dendritic tree of PC during the second postnatal week (Yamada et al. 2000).

To analyze LPP3 expression during BG and cerebellum development, we used a reporter allele, immunohistochemistry and immunofluorescence in cerebella from E16 to postnatal day 10 (P10) individuals (Fig. 2). At E16, expression of LPP3 was restricted to two domains, at the most mid-rostral region and at the ventricular and intermediate zones (Fig. 2A asterisks); this expression pattern is in agreement with the ventricular origin of BG precursors. Around the perinatal period, a strong LPP3 expression domain was observed in the junction between the rostral-most part of the cerebellum primordium and the developing velum medullaris (Fig. 2B–C). Furthermore, LPP3-positive cells in the PCL became initially evident in the rostral lobules and forming posterior fissures. Appearance of LPP3-positive cells with radial processes that traverse the EGL correlated with the degree of alignment of BG into the PCL at this stage (Yamada et al. 2000), supporting its identity as BG. In addition, a weak LPP3-expressing domain was observed in the anterior medulla of early postnatal cerebella (Fig. 2B inset), which extended to the entire medulla by P4 (Fig. 2D inset). At P4, LPP3-expressing BG cells arranged along the entire PCL (Fig. 2D) while the positive cells found in the medulla disappeared as development progressed, in agreement with disappearance of immature BG from this area. By P10, LPP3 expression was essentially identical to the adult stage except for the presence of LPP3-positive radial processes that still cross the remaining EGL (Fig. 2E–F). The developmental expression pattern of LPP3 described indicate that this enzyme is weakly expressed in BG precursors (E16), becomes highly expressed in immature and mature BG cells (perinatal stage onwards) and reflects the dynamic transformation that this cell type undergoes during postnatal development.

Lack of LPP3 alters S1P metabolism and $S1P_1$ expression in the cerebellum

Due to the early embryonic lethality of *Ppap2b* null mutants we used a genetic approach to conditionally inactivate *Ppap2b* in neural precursors. The $Ppap2b^{tm3Stw}$ conditional allele (*f*) (Escalante-Alcalde et al. 2007) and a *Nestin::Cre* transgenic (Tronche et al. 1999) were used to inactivate the gene in neuron-glial progenitors from around E11 onwards (stage at which the transgenic broadly expresses Cre in nervous system). *Nestin::Cre*-mediated neural inactivation of *Ppap2b* resulted in viable and fertile mice, indicating that neuron-glial expression of LPP3 after E11 is not essential, however mice were ~20% smaller than controls. The highly efficient recombination of *Ppap2b* locus in the cerebellum of adult *Nestin::Cre;* $Ppap2b^{tm3Stw/tm3Stw}$ animals (from here onwards referred as CKO in the text and $Ppap2b^{N\Delta flox/N\Delta flox}$ or simply $\Delta f/\Delta f$ in the figures) was corroborated by PCR of genomic DNA (data not shown), western blot and immunofluorescence (Fig. 3A). Out of the

three LPPs found in mice, LPP3 is the only abundantly expressed in the adult cerebellum (Fig. S1), thus inactivation of *Ppap2b* should render changes in concentrations of their lipidic substrates and/or products. We performed lipid profiling by LC-MS/MS in CKO as in control cerebella and found that the level of S1P was consistently elevated in cerebellar tissue samples from CKO mice in comparison to controls, while LPA and PA or LPC (the latter not an LPP substrate) showed no statistical differences (Figs. 3B, S2A). Aside from our previous observations showing that LPA, PA and DAG levels are modified in null LPP3 mouse embryo fibroblasts *in vitro* (Escalante-Alcalde et al. 2003), the physiological role of LPP3 in lipid phosphate metabolism *in vivo* was largely unexplored. Our results indicate that LPP3 is a functional S1P phosphatase in the mouse cerebellum and is required for maintaining the appropriate levels of this lipid in that structure.

The presence and role of S1P in the cerebellum has been slightly studied: Sphingosine kinase (SPHK) activity in the CNS is highest in the cerebellum (Blondeau et al. 2007), SPHK1 expression has been found compartmentalized in some PC parasagittal stripes (Terada et al. 2004) and S1P can also be synthesized by cerebellar astrocytes and granule cells (Anelli et al. 2005). Furthermore, S1P promotes the proliferation of cerebellar astrocytes (Bassi et al. 2006) and produces Ca^{2+} signaling in cerebellar astrocytes and differentiated granule cells (Giussani et al. 2007). Between the mRNAs coding for S1P receptors expressed in the adult mouse cerebellum, the most abundant in the PCL and in the entire cerebellum is for the receptor 1 ($S1P_1$/*S1pr1*, Fig. S1). In addition, transcripts coding for proteins involved in S1P signaling ($S1P_1$ and SPHK2) have been found highly enriched in mouse BG cells at P30 (Koirala and Corfas 2010) suggesting that BG cells are a major contributor to S1P signaling in the cerebellum. To date no information exists regarding the abundance and distribution of $S1P_1$ in the mouse cerbellum, thus we performed $S1P_1$ immunofluorescence and immunohistochemistry. In control cerebella $S1P_1$ was primordially detected in the ML with a pattern similar to that of LPP3 and Glast implicating that its expression is mainly in BG; however due to the origin of the antibodies we were only able to show co-localization between $S1P_1$ and Glast (Figs. 3C and S2C). This result indirectly shows that $S1P_1$ and LPP3 are at least located in the same plasma membrane domains of BG cells. Surprisingly, when we analyzed the expression of $S1P_1$ in CKO cerebella, a pronounced decrease in the amount of $S1P_1$ in the ML was observed in the adult as well as in the developing postnatal cerebellum (Fig. 3C and S2D–G). To rule out a possible artifact of the antibody staining we performed western blot, which confirmed our immunostaining results (Fig. 3D) and pointed to a down-regulation of the receptor in the mutant cerebellum. The amount of *S1pr1* mRNA was unaltered in the CKO, which suggested that the decrease in the amount of receptor is due to degradation (Fig. S2B). Given the dramatic decrease in the amount of $S1P_1$, we explored whether the CKO adult cerebellum, showed global changes in the activation of some $S1P_1$ downstream signaling molecules. While AKT activation was diminished in CKO cerebellum extracts vs. controls, activation of ERK1/2 was increased. On the other hand, we were unable to detect consistent differences in the activation of PKC (Fig. S2H). Altogether these data suggest that a sustained activation of $S1P_1$, due to the increase in extracellular S1P availability, is responsible for the internalization and degradation of this receptor in CKO animals, even during early postnatal cerebellum development. Experiments in isolated BG cells will be required to further dissect the signaling consequences of the absence of LPP3 in this system, however our results clearly demonstrate the requirement of LPP3 expressed in BG for the regulation of S1P metabolism/signaling in the cerebellum *in vivo*.

Neural inactivation of Ppap2b produces mild defects in motor coordination

The cerebellum is the structure that regulates learning and coordination of skilled movements. Thus we subjected control and CKO animals to neurological tests to reveal

motor dysfunctions. On the Rotarod, which measures coarse motor performance, one month-old CKO mice showed significant smaller latency periods to fall at 20 and 30 rpm (Fig. 4A). On the fixed bar test, which reveals fine motor coordination defects particularly of the hindlimbs, performance of CKO mice was considerably affected in 100% of individuals. Although they were able to stay and move along the beam, they showed grasping and pulling movements with the forepaws and dragged the hindlimbs on the beam (Fig. 4B). No signs of worsening were found in one year-old mice, indicating that the motor dysfunction was not progressive at least up to this age. These results suggested possible alterations in the cerebellum physiology.

LPP3 deficiency in the cerebellum produces foliation defects and alters BG arrangement and cytoarchitecture

One source of altered cerebellar function corresponds to malformations with developmental origin (Chizhikov and Millen 2003). Since BG plays fundamental roles in cerebellum development we analyzed the structure of control and CKO adult cerebella and found alterations in the foliation pattern of mutants (Fig 5, S3). Macroscopic analysis showed a pronounced hypotrophy of folias IV–V (Fig. S3) and IX (data not shown). Histological analysis of sagittal sections at the mid vermis from CKO cerebella revealed: i) hypoplasia of folia III; ii) a less pronounced precentral fissure; iii) reduced folia IV–V (culmen); iv) reduced or absent intercrural fissure in folia VI/VII and v) underdeveloped folia IX (uvula) with absent uvular sulcus (Fig. 5 A, E). Also, in the most rostral area of the vermis, near the junction to the velum medullaris, a lingular-like sulcus with an abnormal accumulation of cells in the dorsal side of the molecular layer was observed (Fig. 5E).

To further study whether LPP3 deficiency affected the cytoarchitecture of BG or other cerebellar cell type in the adult stage, we analyzed PC, interneuron and BG arrangement, density and morphology at this stage. Morphology and density of PC in CKO were not evidently affected (Fig. 5B, F and I), however a mild disorganization of PC somas was sometimes observed in earlier stages (Fig. 6C–D). The number and distribution of interneurons along the ML were neither affected (Fig. 5B, F and I). In contrast, BG numbers, arrangement and morphology were evidently altered in CKO adult animals (Fig. 5C–D, G–I). While in control cerebella the radial processes of BG had the typical palisade distribution, with their end feet at the pial surface and their somas located at the PCL, in the CKO the radial processes looked thicker and disorganized, and many of them did not reach the pial surface. Furthermore, their somas looked less organized within the PCL and were frequently misplaced in the ML. BG was 41.6% less abundant in the CKO PCL than in controls and 11% of total BG cells were located in the ML of CKO animals. These abnormalities were found along the ML regardless of the folia observed. Confocal analysis revealed an apparent increase in the intensity of GFAP so we performed western blot of cerebellum protein extracts using antibodies against GFAP and two other BG markers, BLBP and Glast. Remarkably, while Glast showed no difference, BLBP and GFAP were increased 2- and 1.5-fold respectively, in CKO extracts versus controls (Fig. S4). The exact meaning of this result remains to be established, however it is worth noting that up-regulation of GFAP is considered a landmark of reactive gliosis, which is normally associated with neural damage.

To address how early BG is affected in the CKO, we analyzed its positioning and morphology during postnatal cerebellum development. We found an abnormal arrangement of BG somas in the developing PCL as early as P4 (Fig. 6A–B), while ectopic BG somas in the ML were evident at P10–15 (Fig. 6C–D). At the latter stages, besides the disarrangement of BG somas, their radial processes were already thicker, tortuous and many of them did not reach the pial surface. Furthermore the complexity of their fine lateral processes was apparently reduced. In addition, a decrease in the density of BLBP-positive somas in the

PCL was apparent in these early stages (Fig. 6A–D), suggesting a decrease in BG numbers even during early postnatal stages.

Rostral-most defects are associated to alterations in LPP3-expressing glial cells

As mentioned earlier, an abnormal accumulation of cells was observed in the dorsal side of the molecular layer in the most rostral area of the vermis (Fig. 5E). The composition of this cumulus of cells was heterogeneous and formed by interneurons, PC, proliferating and postmitotic granular cells, astrocytes and BG cells (Fig. S5 A–E). In E17.5 mouse embryos, the medial cerebellum is delimited at the rostral end by the extension of the EGL, which ends almost at the isthmus in the mid-hindbrain boundary (MHB). During the next few days, an isthmic-derived structure develops and forms a wide sheet of cells devoid of neurons, the velum medullaris (VM). This structure links the anterior vermis to the inferior culliculus. To gain further insight into the origin of this rostral abnormality we analyzed mid-rostral cerebellum development in P0–P1 individuals. Sections at the mid vermis region were analyzed to observe the extension of EGC rostral migration, the location of PC and the structure of the VM. As shown in figure S5 (F–G), in P0 CKO cerebellum the EGL extended rostrally up to the VM and was mildly curved. Moreover, the morphology of BLBP-positive radial glia, including BG cells, was altered: in the cerebellar area, radial processes that crossed the EGL were enlarged while in the velum area showed signs of disorganization, leading to an apparent disruption of the glia limitans. At P1 (Fig. S5 H–I) the curvature of the EGL was more pronounced even folding the most anterior end of this layer. Remarkably, a cumulus of calbindin-positive cells, presumably PC, was already observed in the dorsal side of this sulcus-like structure. Two possible cellular mechanisms could account for the formation of this abnormal structure, a localized increase in the proliferation rate of EGC or defective elongation of the velum medullaris. We found no evidence of increased proliferation rate of EGC in this area (Fig. 7C) suggesting that the sulcus-like structure arises due to defective elongation of the VM. Altogether these data suggest that in the perinatal cerebella, LPP3-expressing cells (presumably radial glia) in the velum and in the junction between the velum and the anterobasal lobe of the vermis (white arrowheads in Fig. 2B–C) play a fundamental role in controlling the elongation of the velum and proper formation of the glia limitans in this area.

Deficiency of LPP3 in BG produces proliferation defects and EGC delayed migration

As noted, adult CKO cerebellum showed hypoplasia and reduction or disappearance of fissures and sulci. These phenotypes are frequently associated to defects in migration, proliferation and/or survival of granule cells (Chizhikov and Millen 2003). In the mouse, EGC use the radial processes of BG cells as scaffolds to reach the IGL from around the perinatal stage onwards being the peak of migration between P8 and P10 (Yacubova and Komuro 2002). Since LPP3-deficient BG cells showed morphological defects from early stages of cerebellum development, it was possible that EGC had secondary developmental abnormalities associated to this phenotype (Rakic and Sidman 1973). We found that in CKO cerebella, between P10–P15, the EGL was thicker than in control littermates (Figs. 6C–D, 7A–D); however in adult animals no sign of remaining EGC was detected (Fig. 5A, E). This observation suggested a delayed migration of EGC in the CKO. To test this possiblility, we analyzed the amount and distribution of PCNA- and p27-positive cells (proliferating and postmitotic premigratory EGC, respectively) in P15 cerebella. In regions where a few PCNA-positive cells were observed in fissures of control cerebella, the corresponding areas in CKO showed a large amount of PCNA positive cells (Fig. 7A–B). Furthermore, in areas where proliferating EGC were still found in controls (i.e. folias VI–VII and X), the thickness of the EGL positive to PCNA was larger in CKO (not shown). Similar observations were found in regard to the thickness of EGL with postmitotic cells (p27-positive) in the CKO animals vs. controls (Fig. 7C–D). Indication of delayed migration of EGC was strongly

suggested by the reduction of p27-positive fusiform cells found in the molecular layer of CKO cerebella compared to control animals (arrowheads in Fig. 7C–D).

Delayed granule cell migration on its own might not account for the hypoplastic/foliation phenotypes found in mutants suggesting additional alterations in proliferation and/or cell death rates during CKO cerebellum development. To test this hypothesis, we performed a time-course analysis of proliferation (phospho-Histone-H3) and cell death (TUNEL) in CKO vs. control cerebella between P0–P15. Remarkably, a decrease in mitotic cells and an increase in TUNEL-positive cells were observed in CKO cerebella in a temporal and regional fashion (Fig. 7E–H). At P0–1, proliferating cells in the EGL were not altered while in the PCL a decrease in mitotic cells (18%) was observed in CKO. By P4 (estimated to be near the proliferation peak of BG cells in the mouse, Shiga et al, 1983) a significant decrease (33%) in the number of mitotic cells was observed in the EGL (principally in folias of the anterior lobe) and in the PCL (28%; principally in folias IV–VIII). Between P0–P4, most of the cells that proliferate in the PCL are BG, implying that this cell type is the one affected by the absence LPP3 in this layer. At P7–8, no differences in proliferation were found in the PCL (BG already cease proliferation at the stages), but a 17% reduction in proliferating cells in the EGL was observed principally in folias III and X. Finally, a considerable increase (2.6 fold) in TUNEL-positive cells was detected in the EGL and ML of CKO cerebella at P15. This correlated with the delayed EGC migration observed at this stage, suggesting that the ectopically differentiated GCs that do not reach the internal granule layer die. Thus foliation defects seem originated by a combination of reduced proliferation, increased cell death and delayed migration of EGC, all secondary to BG defects.

In vitro and in vivo treatments with a $S1P_1$ functional antagonist, partially phenocopies developmental cerebellum alterations

We finally explored if S1P/$S1P_1$-signaling alterations could contribute to the developmental defects observed. FTY720 is a S1P receptor modulator, which is phosphorylated by sphingosine kinases *in vivo* to form the active compound FTY720-P. The latter causes internalization and degradation of $S1P_1$ expressed at the plasma membrane, thereby working as a $S1P_1$ functional antagonist (Brinkmann 2009; Nixon 2009). Due to its lipophilic nature FTY720 crosses the blood-brain barrier (Foster et al. 2007) and recent evidence suggests that it can act in CNS cells including astrocytes (Miron et al. 2008). Taking advantage of the properties and mechanism of action of this drug on $S1P_1$, we performed slice organotypic cultures of P7 wildtype cerebella incubated for 48 hrs in the presence or absence of 100 nM FTY720 and then BG morphology was analyzed by immunofluorescence against BLBP. As shown in figure 8, FTY720 treatment produced alterations in BG morphology, including thickening of radial processes and a mild reduction in the complexity of the fine lateral processes, although the morphological changes were not as severe as those found in cultured LPP3 deficient cerebella (Fig. 8A–D). To obtain a chronic effect of the drug through cerebellum development we then treated pups between P3–P14 with FTY720 at a dose used to treat a mouse model of multiple sclerosis (Foster et al. 2009) (0.3 μg/g of body weight, daily i.p. injection) and then assessed BG morphology and arrangement, $S1P_1$ expression and EGC proliferation. In FTY720 treated-animals (n=4), BG radial processes were thicker than in controls along the entire ML while BG soma arrangement was just regionally perturbed (Fig. 8E, F). In folia X, which is one late-developing folia, BG somas were not homogeneously aligned within the PCL. In addition some ectopic somas were found within the ML of this folia and with less frequency in other folias. BG ectopia was never observed with the same frequency in animals treated with vehicle (n=3) (Fig. 8E, F). The low expressiveness of phenotypes observed could be due to the relatively low dose of drug used and/or the short and late window of time (in terms of cerebellum development) in which the treatment was applied. We indirectly analyzed the effectiveness of FTY720 treatment

through the detection of $S1P_1$ expression in control and treated cerebellum sections by confocal microscopy under the same optical parameters. $S1P_1$ expression was reduced by FTY720 treatment although not to the extent found in CKO cerebella (compare Figs. 3C, D and 8G, H). Furthermore, the regions where a more prominent decrease in $S1P_1$ expression was observed correlated with folia showing more pronounced alterations. Finally, the thickness of EGL positive to PCNA in the intercrural fissure of treated animals was increased (27%) as occurred in the CKO (Fig. 8I, J), although in a more moderate fashion. Altogether these results strongly suggest that alteration in S1P metabolism/signaling, due to the lack of LPP3 activity in BG cells, contribute to the developmental abnormalities found.

DISCUSSION

Although it has been recently reported an important role for an LPP-related protein, PRG1/LPPR4, in hippocampal excitability (Trimbuch et al. 2009) no information regarding the participation of bona fide LPPs in the function and development of the CNS exists. Abundant *Ppap2b* transcription has been found in neurogenic areas of the rat brain (Suzuki et al. 1999), however the exact identity of the cells that express LPP3 in these regions remains unidentified. Transcriptional profiling studies in human brain showed that *Ppap2b* is within the top ten genes with highest membership to a group enriched in markers of astrocytes, which in turn have a significant overlap to a group rich in neurogenic markers (Oldham et al. 2008), suggesting that LPP3 is abundantly expressed in a population of astrocytes involved in neurogenic processes. Supporting this notion we found that in developing and adult cerebellum, LPP3 is restricted to BG astrocytes and its precursors, with a highly strong expression found in immature and mature BG (from P0 onwards), which have been found to possess stem cell-like properties (Alcock and Sottile 2009).

The subcellular distribution of LPP3 in BG was highly specific showing a close resemblance to the distribution of the neurotransmiter transporter Glast, which is involved in fast glutamate removal during synaptic events (Takayasu et al. 2009). This suggested the participation of LPP3 in some aspects of neuron-glia communication through the dephosphorylation of extracellular bioactive lipids such as S1P and LPA. Since these lipids lead to a variety of effects in neurons and astrocytes we designed strategies to conditionally inactivate LPP3 gene function in neuroglial lineages.

We demosntrated that lack of LPP3 protein/activity in BG produces an increase in the concentration of S1P and the down-regulation of $S1P_1$ in adult and developing cerebellum, indicating that LPP3 in BG contributes to the regulation of S1P metabolism and signaling in this structure *in vivo*. These data, in addition to the expression of S1P synthesizing enzymes in the cerebellum, as well as the described effects of S1P in some cerebellar cell types, suggested that the tight regulation of S1P metabolism/signaling might be relevant for some aspects of cerebellum development and/or physiology.

In this work we characterized the cerebellar alterations produced by the lack of LPP3 expression in the nervous system: 1) appearance of an abnormal lingular-like sulcus with ectopic neurons, in the most rostral domain of the vermis; 2) hypoplasia of folias and reduction or disappearance of fissurae/sulci and 3) abnormal morphology and arrangement of BG cells. Most of these abnormalities have a developmental origin and could be attributed to changes in cell morphology and/or density of LPP3-positive radial glia as will be discussed immediately after.

In the case of the sulcus with ectopic cells, abnormal development of the velum medullaris can afford for this phenotype. It has been suggested that this structure arises from active proliferation of cells in the VZ and the posterior retraction of the anterior end of the vermis

causing the velum to delaminate from the anterior cerebellum and expand (Louvi et al. 2003). Based on the expression pattern of LPP3 and the phenotypic analysis of CKO, we propose that in the perinatal cerebella, LPP3-expressing cells in the velum and in the junction between the velum and the anterobasal lobe of the vermis (Fig. 2) play a fundamental role in controlling the elongation of the velum and proper formation of the glia limitans in this area. In the absence of LPP3, abnormal “contraction/tension” of cells in the velum area folds the anterior end of the vermis and drag some cells, accounting for ectopic neurons found in this area. Alternatively, cells might move farther as a consequence of the loss of a restrictive signal at the MHB imposed by LPP3 or the phenotype might be the consequence of a mild midline fusion defect, but these possibilities have to be tested.

LPP3 deficiency modifies cerebellum foliation in part through alterations in EGC proliferation in a regional and temporal fashion. It is established that proliferation kinetics of EGC is controlled by SHH produced from PC and modulated by several factors (Vaillant and Monard 2009). Our evidence shows that LPP3 is not obviously expressed in PC or EGC, thus the alteration on EGC proliferation in the CKO should be an indirect consequence of the absence of LPP3 in BG cells. One possibility is that the decrease in BG cell-density affects one of the components that positively regulate SHH signaling in the EGC. This notion is supported by the regional decrease in BG proliferation observed during CKO cerebellum development, which correlates with areas showing a broader decrease in EGC proliferation (i.e. at P4). A close correlation in the spatial-temporal patterns of proliferative activity between these cell types has been also suggested for the rat (Shiga et al. 1983). The possibility that foliation defects are a consequence of the general reduction in size of CKO animals is unlikely, as the change in size does not seem to be a critical factor in determining the pattern of cerebellar foliation (Millen et al. 1994)

LPP3-deficiency in BG cells reduces their proliferation partly accounting for the decrease in BG density in later stages. Since S1P released by cerebellar astrocytes induces its proliferation (Bassi et al. 2006), it is possible that the accumulation of extracellular S1P caused by the absence of LPP3, induces the desensitization/degradation of S1P receptors that mediate BG proliferation. In support of this notion is the early down-modulation of $S1P_1$ found in the CKO cerebellum from P4, which correlates with the stage in which more effects on BG proliferation were found (Figs. 7, S2).

A great body of evidence supports that alterations in the cytoarchitectonic features of BG cells may produce alterations in EGC migration due to abnormal scaffold formation (Eiraku et al. 2005; Lin et al. 2009; Qu and Smith 2005; Rakic and Sidman 1973; Weller et al. 2006). In our LPP3 CKO cerebella, EGC migration is delayed without affecting their differentiation since expression of p27 in the inner EGL is normal. However, cell death of differentiated GC trapped in the EGL and ML was suggested by the increase in TUNEL positive cells found in these areas in CKO cerebella at P15. Thus, foliation defects found in LPP3 deficient cerebella arise from a combination of events, namely, reduction in the amount of EGC due to reduced proliferation, a delay in EGC migration and a late increase in GC death.

Posterior to the migration of BG somas from the ventricular zone through the cerebellar medulla, they arrange in an epithelium-like lining in the PCL. Lack of LPP3 also produces alterations in the arrangement of BG into this layer. This phenotype, aside from changes in the BG cytoarchitecture and delayed EGC migration, has been associated to disrupted activation of the Notch signaling, a pathway involved in intercellular interaction (Eiraku et al. 2005; Komine et al. 2007; Weller et al. 2006). Whether the absence of LPP3 is affecting the interactions between PC and BG through the alteration of the Notch signaling or other

mechanism regulating intercellular interaction is an intriguing idea that remains to be analyzed.

As previously highlighted, the broad phenotypic alterations found in the LPP3 CKO cerebellum seemed mainly associated to alterations in the cytoarchitectonic features of BG. S1P-mediated signaling regulates cell adhesion and/or cell shape in glial cells (Mullershausen et al. 2007; Tas and Koschel 1998) and cerebellar astrocytic proliferation *in vitro* (Bassi et al. 2006). Since LPP3 and $S1P_1$ are extremely abundant in BG (this work and Nishimura et al. 2010), and that lack of LPP3 increases the availability of S1P and down-regulates $S1P_1$ in BG, it was possible that most of the abnormalities found in this cell type originated from altered S1P/$S1P_1$ metabolism/signaling. The similar changes in cell morphology and alterations in soma arrangement found in BG, in addition to the significant reduction in the expression of $S1P_1$ in our *in vitro* and *in vivo* pharmacological treatments with the S1P receptor modulator FTY720, strongly supports this hypothesis. The phenotypic rescue with the conditional expression in BG of a mutant version of $S1P_1$ that cannot be internalized in our *Nes-Cre;Ppap2b*^{Floxed} background, or the phenocopy of the phenotypes with the conditional ablation of $S1P_1$ in this particular cell type will ultimately clarify this issue.

Lack of LPP3 in the nervous system also produces a mild motor coordination defect. Establishing whether structural or electrophysiological abnormalities in the cerebellum are responsible for this motor dysfunction will require further investigation. However, it is suggestive that the anterior lobule of the cerebellum, the region that primordially controls the movement of posterior appendages (Manni and Petrosini 2004), is the most altered in our mice. Alternatively, modifications in lysophospholipid signaling due to the absence of LPP3 could originate electrophysiological alterations that compromise information processing of the cerebellum. For instance, altered S1P-mediated signaling might affect glutamatergic neurotransmission (Sim-Selley et al. 2009). Our neural specific LPP3 knockout constitutes a suitable model to analyze the role of LPP3 and lysophospholipids in BG cell function and cerebellar physiology in general.

Finally, the tight functional connection between LPP3 and the regulation of $S1P_1$ expression at the plasma membrane is highly significant since the down-regulation of this receptor is the mechanism by which the immunomodulator FTY720 works in the treatment of some autoimmune diseases (Brinkmann 2009; Nixon 2009). In this sense, it will be interesting to explore if regulating the expression or activity of LPP3 could also contribute to the treatment of this kind of diseases.

Supplementary Material

Refer to Web version on PubMed Central for supplementary material.

Acknowledgments

The authors wish to thank to Drs. Massieu, Chagoya, Salceda and Tapia for reagents and equipment; Drs. Rosenbaum and Sánchez for critical reading of the manuscript; the Microscopy Unit and Animal facility for technical support. This work was supported by CONACyT 39995, 53777; PAPITT IX208504, IN216009; NIH R01GM50388 and 1P20RR021954. A.L-J and R.S-S. received a fellowship from CONACyT. This work constitutes a partial fulfillment of A.L-J to obtain the Ph.D. degree in Biomedical Sciences-PDCB/UNAM.

REFERENCES

Albers H, Dong A, van Meeteren LA, Egan D, Sunkara M, van Tilburg E, Schuurman K, van Tellingen O, Morris AJ, Smyth SS, et al. Boronic acid-based inhibitors of the LPA-generating

phospholipase, autotaxin, reveal rapid turnover of LPA in the circulation. Proc Natl Acad Sci (USA). 2010 in press 2010.

Alcock J, Sottile V. Dynamic distribution and stem cell characteristics of Sox1-expressing cells in the cerebellar cortex. Cell Res. 2009; 19(12):1324–1333. [PubMed: 19823196]

Anelli V, Bassi R, Tettamanti G, Viani P, Riboni L. Extracellular release of newly synthesized sphingosine-1-phosphate by cerebellar granule cells and astrocytes. J Neurochem. 2005; 92(5): 1204–1215. [PubMed: 15715670]

Bassi R, Anelli V, Giussani P, Tettamanti G, Viani P, Riboni L. Sphingosine-1-phosphate is released by cerebellar astrocytes in response to bFGF and induces astrocyte proliferation through Gi-protein-coupled receptors. Glia. 2006; 53(6):621–630. [PubMed: 16470810]

Blondeau N, Lai Y, Tyndall S, Popolo M, Topalkara K, Pru JK, Zhang L, Kim H, Liao JK, Ding K, et al. Distribution of sphingosine kinase activity and mRNA in rodent brain. J Neurochem. 2007; 103(2):509–517. [PubMed: 17623044]

Bordey A, Sontheimer H. Modulation of glutamatergic transmission by bergmann glial cells in rat cerebellum in situ. J Neurophysiol. 2003; 89(2):979–988. [PubMed: 12574474]

Brindley, DN.; Bräuer, A. Lipid Mediators and Modulators of Neural Function: Lysophosphatidate and Lysolipids. New York USA: Springer Sciences; 2009. p. 289-310.

Brindley DN, Pilquil C, Sariahmetoglu M, Reue K. Phosphatidate degradation: phosphatidate phosphatases (lipins) and lipid phosphate phosphatases. Biochim Biophys Acta. 2009; 1791(9):956–961. [PubMed: 19250975]

Brinkmann V. FTY720 (fingolimod) in Multiple Sclerosis: therapeutic effects in the immune and the central nervous system. Br J Pharmacol. 2009; 158(5):1173–1182. [PubMed: 19814729]

Chizhikov V, Millen KJ. Development and malformations of the cerebellum in mice. Mol Genet Metab. 2003; 80(1–2):54–65. [PubMed: 14567957]

Dennis J, Nogaroli L, Fuss B. Phosphodiesterase-Ialpha/autotaxin (PD-Ialpha/ATX): a multifunctional protein involved in central nervous system development and disease. J Neurosci Res. 2005; 82(6): 737–742. [PubMed: 16267828]

Eiraku M, Tohgo A, Ono K, Kaneko M, Fujishima K, Hirano T, Kengaku M. DNER acts as a neuron-specific Notch ligand during Bergmann glial development. Nat Neurosci. 2005; 8(7):873–880. [PubMed: 15965470]

Escalante-Alcalde D, Hernandez L, Le Stunff H, Maeda R, Lee HS Jr, Gang C, Sciorra VA, Daar I, Spiegel S, Morris AJ, et al. The lipid phosphatase LPP3 regulates extra-embryonic vasculogenesis and axis patterning. Development. 2003; 130(19):4623–4637. [PubMed: 12925589]

Escalante-Alcalde D, Morales SL, Stewart CL. Generation of a reporter-null allele of Ppap2b/Lpp3and its expression during embryogenesis. Int J Dev Biol. 2009; 53(1):139–147. [PubMed: 19123136]

Escalante-Alcalde D, Sanchez-Sanchez R, Stewart CL. Generation of a conditional Ppap2b/Lpp3 null allele. Genesis. 2007; 45(7):465–469. [PubMed: 17610274]

Estivill-Torrus G, Llebrez-Zayas P, Matas-Rico E, Santin L, Pedraza C, De Diego I, Del Arco I, Fernandez-Llebrez P, Chun J, De Fonseca FR. Absence of LPA1 signaling results in defective cortical development. Cereb Cortex. 2008; 18(4):938–950. [PubMed: 17656621]

Foster CA, Howard LM, Schweitzer A, Persohn E, Hiestand PC, Balatoni B, Reuschel R, Beerli C, Schwartz M, Billich A. Brain penetration of the oral immunomodulatory drug FTY720 and its phosphorylation in the central nervous system during experimental autoimmune encephalomyelitis: consequences for mode of action in multiple sclerosis. J Pharmacol Exp Ther. 2007; 323(2):469–475. [PubMed: 17682127]

Foster CA, Mechtcheriakova D, Storch MK, Balatoni B, Howard LM, Bornancin F, Wlachos A, Sobanov J, Kinnunen A, Baumruker T. FTY720 rescue therapy in the dark agouti rat model of experimental autoimmune encephalomyelitis: expression of central nervous system genes and reversal of blood-brain-barrier damage. Brain Pathol. 2009; 19(2):254–266. [PubMed: 18540945]

Fukushima N, Weiner JA, Chun J. Lysophosphatidic acid (LPA) is a novel extracellular regulator of cortical neuroblast morphology. Dev Biol. 2000; 228(1):6–18. [PubMed: 11087622]

Fukushima N, Weiner JA, Kaushal D, Contos JJ, Rehen SK, Kingsbury MA, Kim KY, Chun J. Lysophosphatidic acid influences the morphology and motility of young, postmitotic cortical neurons. Mol Cell Neurosci. 2002; 20(2):271–282. [PubMed: 12093159]

Fyrst H, Saba JD. Sphingosine-1-phosphate lyase in development and disease: sphingolipid metabolism takes flight. Biochim Biophys Acta. 2008; 1781(9):448–458. [PubMed: 18558101]

Giussani P, Ferraretto A, Gravaghi C, Bassi R, Tettamanti G, Riboni L, Viani P. Sphingosine-1-phosphate and calcium signaling in cerebellar astrocytes and differentiated granule cells. Neurochem Res. 2007; 32(1):27–37. [PubMed: 17151916]

Grosche J, Kettenmann H, Reichenbach A. Bergmann glial cells form distinct morphological structures to interact with cerebellar neurons. J Neurosci Res. 2002; 68(2):138–149. [PubMed: 11948659]

Holtsberg FW, Steiner MR, Furukawa K, Keller JN, Mattson MP, Steiner SM. Lysophosphatidic acid induces a sustained elevation of neuronal intracellular calcium. J Neurochem. 1997; 69(1):68–75. [PubMed: 9202295]

Huang H, Bordey A. Glial glutamate transporters limit spillover activation of presynaptic NMDA receptors and influence synaptic inhibition of Purkinje neurons. J Neurosci. 2004; 24(25):5659–5669. [PubMed: 15215288]

Kimura A, Ohmori T, Ohkawa R, Madoiwa S, Mimuro J, Murakami T, Kobayashi E, Hoshino Y, Yatomi Y, Sakata Y. Essential roles of sphingosine 1-phosphate/S1P1 receptor axis in the migration of neural stem cells toward a site of spinal cord injury. Stem Cells. 2007; 25(1):115–124. [PubMed: 16990586]

Kingsbury MA, Rehen SK, Contos JJ, Higgins CM, Chun J. Non-proliferative effects of lysophosphatidic acid enhance cortical growth and folding. Nat Neurosci. 2003; 6(12):1292–1299. [PubMed: 14625558]

Koirala S, Corfas G. Identification of novel glial genes by single-cell transcriptional profiling of Bergmann glial cells from mouse cerebellum. PLoS One. 2010; 5(2):e9198. [PubMed: 20169146]

Komine O, Nagaoka M, Watase K, Gutmann DH, Tanigaki K, Honjo T, Radtke F, Saito T, Chiba S, Tanaka K. The monolayer formation of Bergmann glial cells is regulated by Notch/RBP-J signaling. Dev Biol. 2007; 311(1):238–250. [PubMed: 17915208]

Lin Y, Chen L, Lin C, Luo Y, Tsai RY, Wang F. Neuron-derived FGF9 is essential for scaffold formation of Bergmann radial fibers and migration of granule neurons in the cerebellum. Dev Biol. 2009; 329(1):44–54. [PubMed: 19232523]

Louvi A, Alexandre P, Metin C, Wurst W, Wassef M. The isthmic neuroepithelium is essential for cerebellar midline fusion. Development. 2003; 130(22):5319–5330. [PubMed: 14507778]

MacLennan AJ, Carney PR, Zhu WJ, Chaves AH, Garcia J, Grimes JR, Anderson KJ, Roper SN, Lee N. An essential role for the H218/AGR16/Edg-5/LP(B2) sphingosine 1-phosphate receptor in neuronal excitability. Eur J Neurosci. 2001; 14(2):203–209. [PubMed: 11553273]

Manni E, Petrosini L. A century of cerebellar somatotopy: a debated representation. Nat Rev Neurosci. 2004; 5(3):241–249. [PubMed: 14976523]

Mathews TP, Kennedy AJ, Kharel Y, Kennedy PC, Nicoara O, Sunkara M, Morris AJ, Wamhoff BR, Lynch KR, Macdonald TL. Discovery, Biological Evaluation, and Structure-Activity Relationship of Amidine Based Sphingosine Kinase Inhibitors. J Med Chem. 2010; 53(7):2766–2778. [PubMed: 20205392]

Millen KJ, Wurst W, Herrup K, Joyner AL. Abnormal embryonic cerebellar development and patterning of postnatal foliation in two mouse Engrailed-2 mutants. Development. 1994; 120(3):695–706. [PubMed: 7909289]

Milstien S, Gude D, Spiegel S. Sphingosine 1-phosphate in neural signalling and function. Acta Paediatr Suppl. 2007; 96(455):40–43. [PubMed: 17391440]

Miriyala S, Subramanian T, Panchatcharam M, Ren H, McDermott MI, Sunkara M, Drennan T, Smyth SS, Spielmann HP, Morris AJ. Functional characterization of the atypical integral membrane lipid phosphatase PDP1/PPAPDC2 identifies a pathway for interconversion of isoprenols and isoprenoid phosphates in mammalian cells. J Biol Chem. 2010; 285(18):13918–13929. [PubMed: 20110354]

Miron VE, Schubart A, Antel JP. Central nervous system-directed effects of FTY720 (fingolimod). J Neurol Sci. 2008; 274(1–2):13–17. [PubMed: 18678377]

Miyake T, Fujiwara T, Fukunanga T, Takemura K, Kitamura T. Glial cell lineage in vivo in the mouse cerebellum. Development Growth & Differentiation. 1995; 37:273–285.

Mizugishi K, Yamashita T, Olivera A, Miller GF, Spiegel S, Proia RL. Essential role for sphingosine kinases in neural and vascular development. Mol Cell Biol. 2005; 25(24):11113–11121. [PubMed: 16314531]

Mullershausen F, Craveiro LM, Shin Y, Cortes-Cros M, Bassilana F, Osinde M, Wishart WL, Guerini D, Thallmair M, Schwab ME, et al. Phosphorylated FTY720 promotes astrocyte migration through sphingosine-1-phosphate receptors. J Neurochem. 2007; 102(4):1151–1161. [PubMed: 17488279]

Nishimura H, Akiyama T, Irei I, Hamazaki S, Sadahira Y. Cellular localization of sphingosine-1-phosphate receptor 1 expression in the human central nervous system. J Histochem Cytochem. 2010; 58(9):847–856. [PubMed: 20566754]

Nixon GF. Sphingolipids in inflammation: pathological implications and potential therapeutic targets. Br J Pharmacol. 2009; 158(4):982–993. [PubMed: 19563535]

Oldham MC, Konopka G, Iwamoto K, Langfelder P, Kato T, Horvath S, Geschwind DH. Functional organization of the transcriptome in human brain. Nat Neurosci. 2008; 11(11):1271–1282. [PubMed: 18849986]

Postma FR, Jalink K, Hengeveld T, Moolenaar WH. Sphingosine-1-phosphate rapidly induces Rho-dependent neurite retraction: action through a specific cell surface receptor. Embo J. 1996; 15(10): 2388–2392. [PubMed: 8665846]

Qu Q, Smith FI. Neuronal migration defects in cerebellum of the Largemyd mouse are associated with disruptions in Bergmann glia organization and delayed migration of granule neurons. Cerebellum. 2005; 4(4):261–270. [PubMed: 16321882]

Rakic P. Neuron-glia relationship during granule cell migration in developing cerebellar cortex. A Golgi and electronmicroscopic study in Macacus Rhesus. J Comp Neurol. 1971; 141(3):283–312. [PubMed: 4101340]

Rakic P, Sidman RL. Weaver mutant mouse cerebellum: defective neuronal migration secondary to abnormality of Bergmann glia. Proc Natl Acad Sci U S A. 1973; 70(1):240–244. [PubMed: 4509657]

Sato K, Tomura H, Igarashi Y, Ui M, Okajima F. Exogenous sphingosine 1-phosphate induces neurite retraction possibly through a cell surface receptor in PC12 cells. Biochem Biophys Res Commun. 1997; 240(2):329–334. [PubMed: 9388477]

Shano S, Moriyama R, Chun J, Fukushima N. Lysophosphatidic acid stimulates astrocyte proliferation through LPA1. Neurochem Int. 2008; 52(1–2):216–220. [PubMed: 17692995]

Shiga T, Ichikawa M, Hirata Y. Spatial and temporal pattern of postnatal proliferation of Bergmann glial cells in rat cerebellum: an autoradiographic study. Anat Embryol (Berl). 1983; 167(2):203–211. [PubMed: 6614505]

Sim-Selley LJ, Goforth PB, Mba MU, Macdonald TL, Lynch KR, Milstien S, Spiegel S, Satin LS, Welch SP, Selley DE. Sphingosine-1-phosphate receptors mediate neuromodulatory functions in the CNS. J Neurochem. 2009; 110(4):1191–1202. [PubMed: 19493165]

Su W, Yeku O, Olepu S, Genna A, Park JS, Ren H, Du G, Gelb MH, Morris AJ, Frohman MA. 5-Fluoro-2-indolyl des-chlorohalopemide (FIPI), a phospholipase D pharmacological inhibitor that alters cell spreading and inhibits chemotaxis. Mol Pharmacol. 2009; 75(3):437–446. [PubMed: 19064628]

Suzuki R, Sakagami H, Owada Y, Handa Y, Kondo H. Localization of mRNA for Dri 42, subtype 2b of phosphatidic acid phosphatase, in the rat brain during development. Brain Res Mol Brain Res. 1999; 66(1–2):195–199. [PubMed: 10095094]

Takayasu Y, Iino M, Takatsuru Y, Tanaka K, Ozawa S. Functions of glutamate transporters in cerebellar Purkinje cell synapses. Acta Physiol (Oxf). 2009; 197(1):1–12. [PubMed: 19583702]

Tas PW, Koschel K. Sphingosine-1-phosphate induces a Ca2+ signal in primary rat astrocytes and a Ca2+ signal and shape changes in C6 rat glioma cells. J Neurosci Res. 1998; 52(4):427–434. [PubMed: 9589387]

Terada N, Banno Y, Ohno N, Fujii Y, Murate T, Sarna JR, Hawkes R, Zea Z, Baba T, Ohno S. Compartmentation of the mouse cerebellar cortex by sphingosine kinase. J Comp Neurol. 2004; 469(1):119–127. [PubMed: 14689477]

Trimbuch T, Beed P, Vogt J, Schuchmann S, Maier N, Kintscher M, Breustedt J, Schuelke M, Streu N, Kieselmann O, et al. Synaptic PRG-1 modulates excitatory transmission via lipid phosphate-mediated signaling. Cell. 2009; 138(6):1222–1235. [PubMed: 19766573]

Tronche F, Kellendonk C, Kretz O, Gass P, Anlag K, Orban PC, Bock R, Klein R, Schutz G. Disruption of the glucocorticoid receptor gene in the nervous system results in reduced anxiety. Nat Genet. 1999; 23(1):99–103. [PubMed: 10471508]

Vaillant C, Monard D. SHH pathway and cerebellar development. Cerebellum. 2009; 8(3):291–301. [PubMed: 19224309]

van Meeteren LA, Ruurs P, Stortelers C, Bouwman P, van Rooijen MA, Pradere JP, Pettit TR, Wakelam MJ, Saulnier-Blache JS, Mummery CL, et al. Autotaxin, a secreted lysophospholipase D, is essential for blood vessel formation during development. Mol Cell Biol. 2006; 26(13):5015–5022. [PubMed: 16782887]

Weller M, Krautler N, Mantei N, Suter U, Taylor V. Jagged1 ablation results in cerebellar granule cell migration defects and depletion of Bergmann glia. Dev Neurosci. 2006; 28(1–2):70–80. [PubMed: 16508305]

Yacubova E, Komuro H. Intrinsic program for migration of cerebellar granule cells in vitro. J Neurosci. 2002; 22(14):5966–5981. [PubMed: 12122059]

Yamada K, Fukaya M, Shibata T, Kurihara H, Tanaka K, Inoue Y, Watanabe M. Dynamic transformation of Bergmann glial fibers proceeds in correlation with dendritic outgrowth and synapse formation of cerebellar Purkinje cells. J Comp Neurol. 2000; 418(1):106–120. [PubMed: 10701759]

Yamada K, Watanabe M. Cytodifferentiation of Bergmann glia and its relationship with Purkinje cells. Anat Sci Int. 2002; 77(2):94–108. [PubMed: 12418089]

Yuasa S. Bergmann glial development in the mouse cerebellum as revealed by tenascin expression. Anat Embryol (Berl). 1996; 194(3):223–234. [PubMed: 8849669]

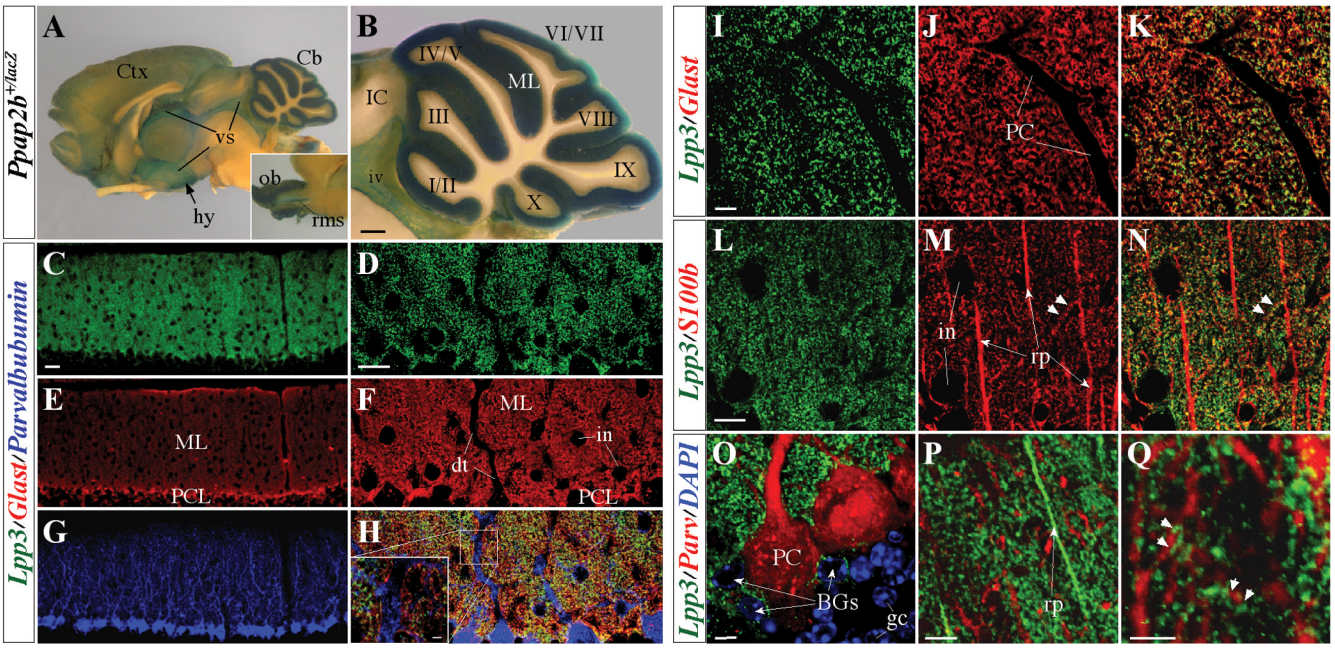

Figure 1. Expression of LPP3 in the adult brain and Bergmann glia

(A–B) β-galactosidase staining (blue) of a *Ppap2b*$^{+/lacZ}$ reporter mouse brain. Confocal images of triple (C–H) or double (I–Q) immunofluorescence in the molecular layer of WT cerebellum, using Abs against the indicated proteins. LPP3 is not expressed in parvalbumin-positive PC (H, O–Q) and S100B-positive radial processes of BG (L–N), but co-localize with Glast-expressing plasma membrane domains (H–K) and S100B-positive lateral braches of BG cells (yellow in N and arrowheads). Few LPP3-positive radial processes were observed near the pial surface (P). Note the close apposition of LPP3-expressing processes to PC dendrites (Q, arrowheads). BGs, Bergmann glia somas; Cb, cerebellum; Ctx, cortex; dt, dendritic tree; gc, granule cells; hy, hypothalamus; IC, inferior coliculus; in, interneurons; iv, fourth ventricle; ML, molecular layer; ob, olfactory bulb; Parv, Parvalbumin; PC, Purkinje cell; PCL, Purkinje cell layer; rms, rostral migratory stream; rp, radial processes; vs, ventricular system; Capitalized roman numbers identify the folias of the cerebellum at the level of the vermis; Scale bars: B, 0.5 mm; C, E, G, 30 μm; D, F, H; 20 μm; H inset, 2 μm.; I, 5 μm; L, 10 μm; O–Q, 5 μm.

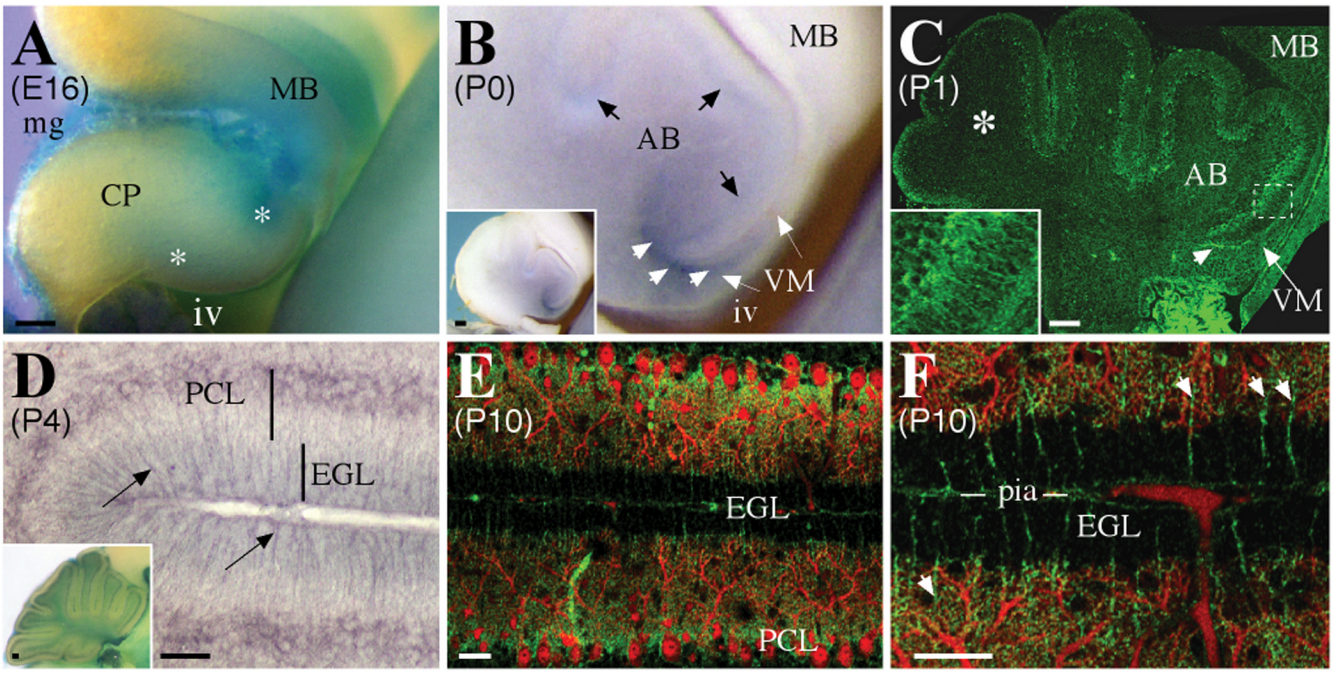

Figure 2. Developmental expression of LPP3 in the cerebellum

Cerebella, at the stages indicated, were stained for β-gal (blue in A and inset in D), for LPP3 by immunohistochemistry (purple; B, D) and immunofluorescence (green, C, E–F) and for Parvalbumin (red, E, F). Asterisks in A show *Ppap2b*^{lacZ} expression domains. White arrowheads in B and C show expression in anterior cerebellum and VM, and black arrows show expression in the developing PCL. Asterisk in C indicates the developing central lobe. Arrows in D and arrowheads in F indicate LPP3-positive radial processes. AB, anterobasal lobe; CP, cerebellum primordium; EGL, external granule layer; iv, fouth ventricle; MB, midbrain; mg, meninges; VM, velum medullaris; Scale bars: A–C and inset in D, 100 μm; D, F, 20 μm; E, 30 μm.

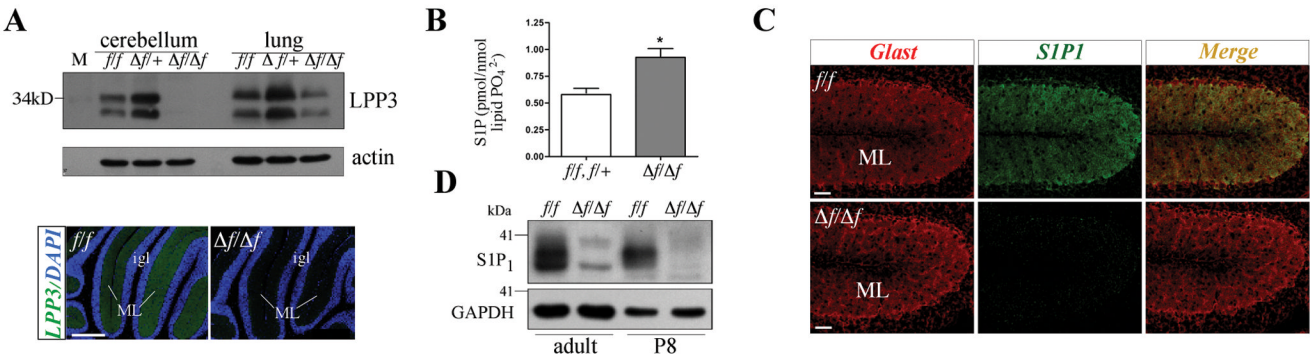

Figure 3. Neural deficiency of LPP3 produces alterations in S1P metabolism and down-regulation of $S1P_1$

A) Western blot and immunofluorescence analyses of LPP3 in total protein extracts of cerebella from *f/f*, Δ*f/+* or Δ*f*/Δ*f* mice. (B) Mass spectrometric analysis of total S1P species extracted from control and CKO cerebella. Mean ± SD (n=3), t test *($p<0.05$). (C) $S1P_1$/Glast double immunofluorescence in sagittal sections at the level of the vermis, from P16 control and CKO cerebellum. (D) Western blot analysis of $S1P_1$ at the stages indicated. igl, internal granule layer; ML, molecular layer. Scale bar: 50 μm.

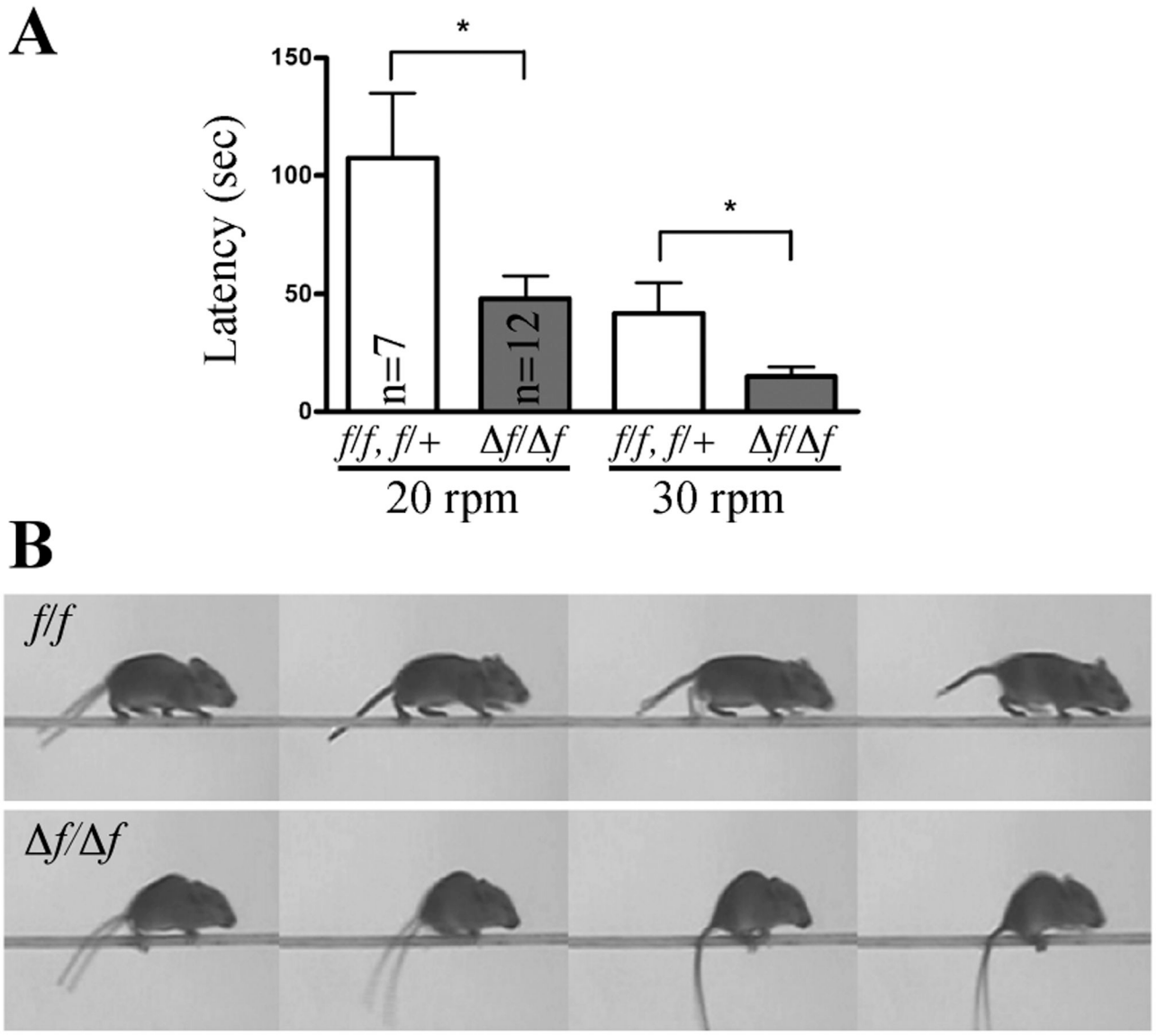

Figure 4. Motor coordination defects in animals lacking neural expression of LPP3

(A) Latency to fall in seconds (sec) on the Rotarod test in control (*f/f*;Δ*f/+*) and CKO (Δ*f*/Δ*f*) animals. Mean ± sem, t test *($p<0.05$). (B) Locomotion pattern of mice on the fixed bar (5 mm diameter).

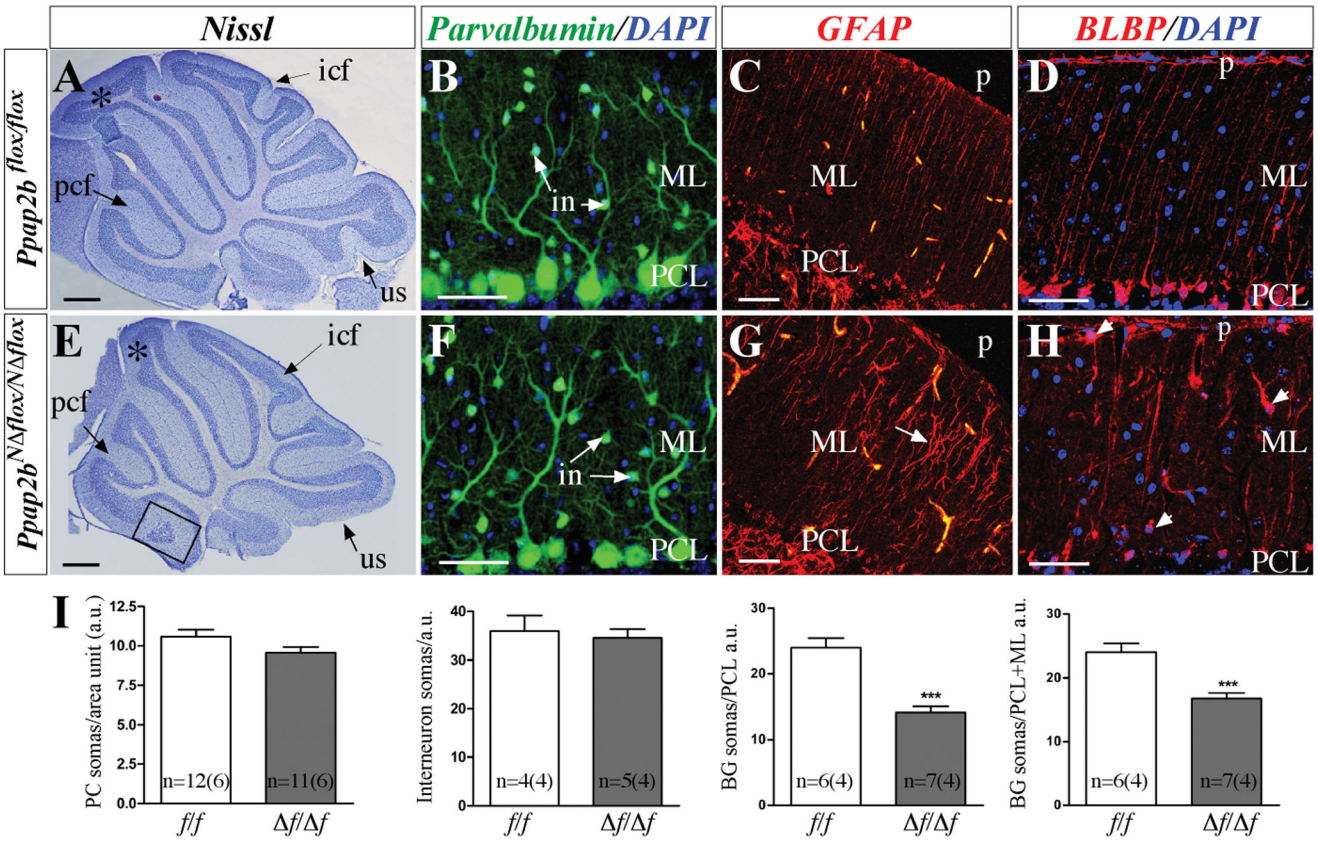

Figure 5. Foliation and BG cytoarchitectonic defects in the LPP3 deficient cerebellum

Histological (A, E) and immunofluorescence (B–D, F–H) analyses in sagittal sections at the mid vermis. Parvalbumin was used to identify Purkinje cells and interneurons (B, F) while GFAP and BLBP were used to identify radial processes or somas and radial processes in BG respectively (C, G; D, H). (I) Quantitative analysis of different cell types densities in the Purkinje cell and molecular layers. Mean ± sem, n=#slices(#animals), t test ***($p<0.001$). Asterisk in A and E indicates the folia IV–V. Rectangle in E shows abnormal lingular-like sulcus. Non-specific fluorescence signal in C, G appears in yellow. Arrow in G show abnormal BG morphology. Arrowheads in H indicate ectopic BG. icf, intercrural fissure; in, interneuron; ML, molecular layer; p, pia; pcf, precentral fissure; PCL, Purkinje cell layer; us, uvular sulcus. Scale bars: A, E, 0.5 mm; B–D, F–H, 50 μm.

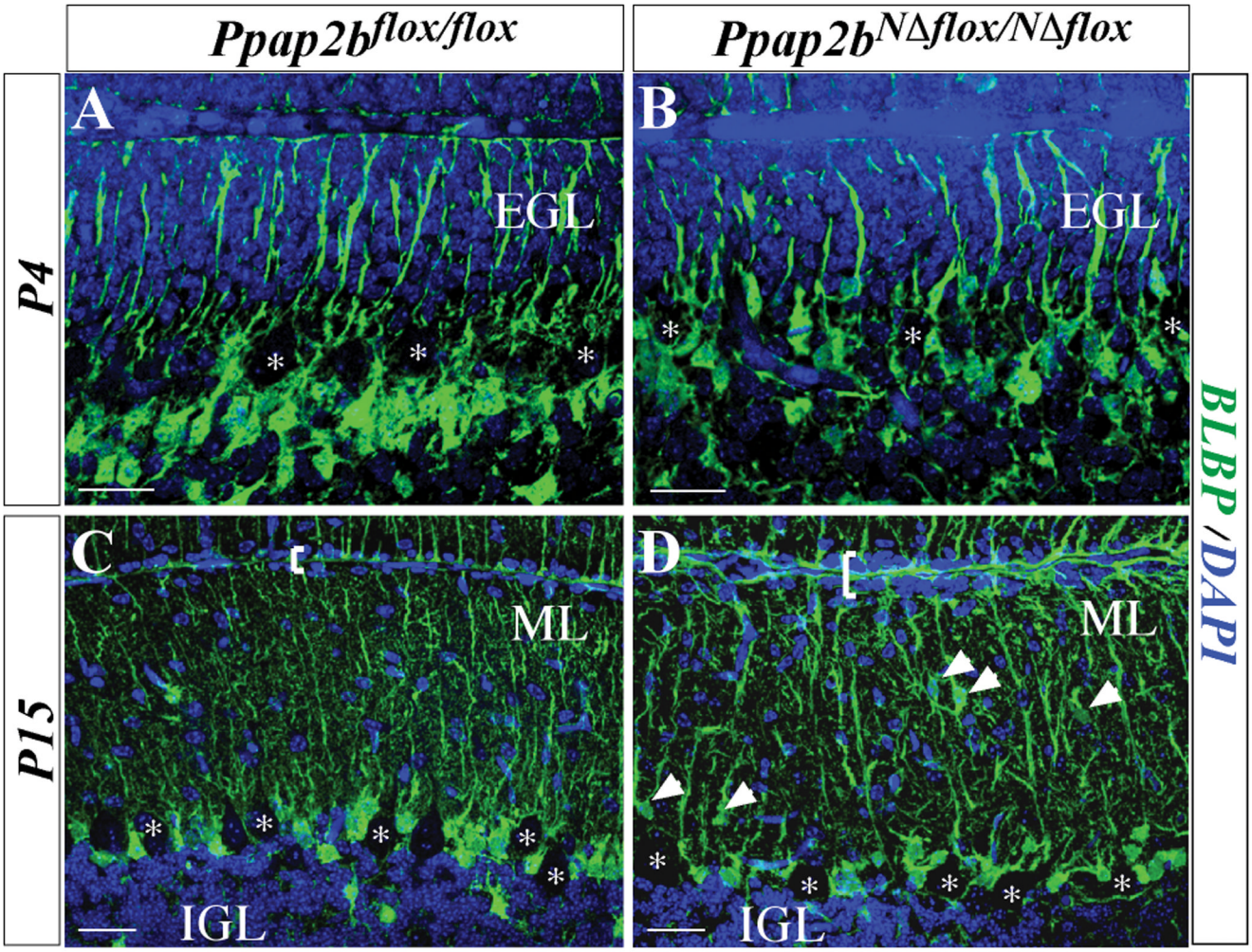

Figure 6. The LPP3-deficient cerebellum shows early alterations in BG cytoarchitecture and arrangement

Sagittal sections from control (A, C) and CKO (B, D) cerebellum at the level of the vermis, processed for immunofluorescence against BLBP (green) at P4 or P15. Note that in P4 mutant sections, BG somas are not as homogeneously arranged below Purkinje cells and appear less abundant; at P15, BG somas are abnormally found in the ML (arrowheads in D). Square brackets in C and D indicate the thickness of EGL. IGL, internal granule layer; *, Purkinje cells. Scale bar: 30 μm.

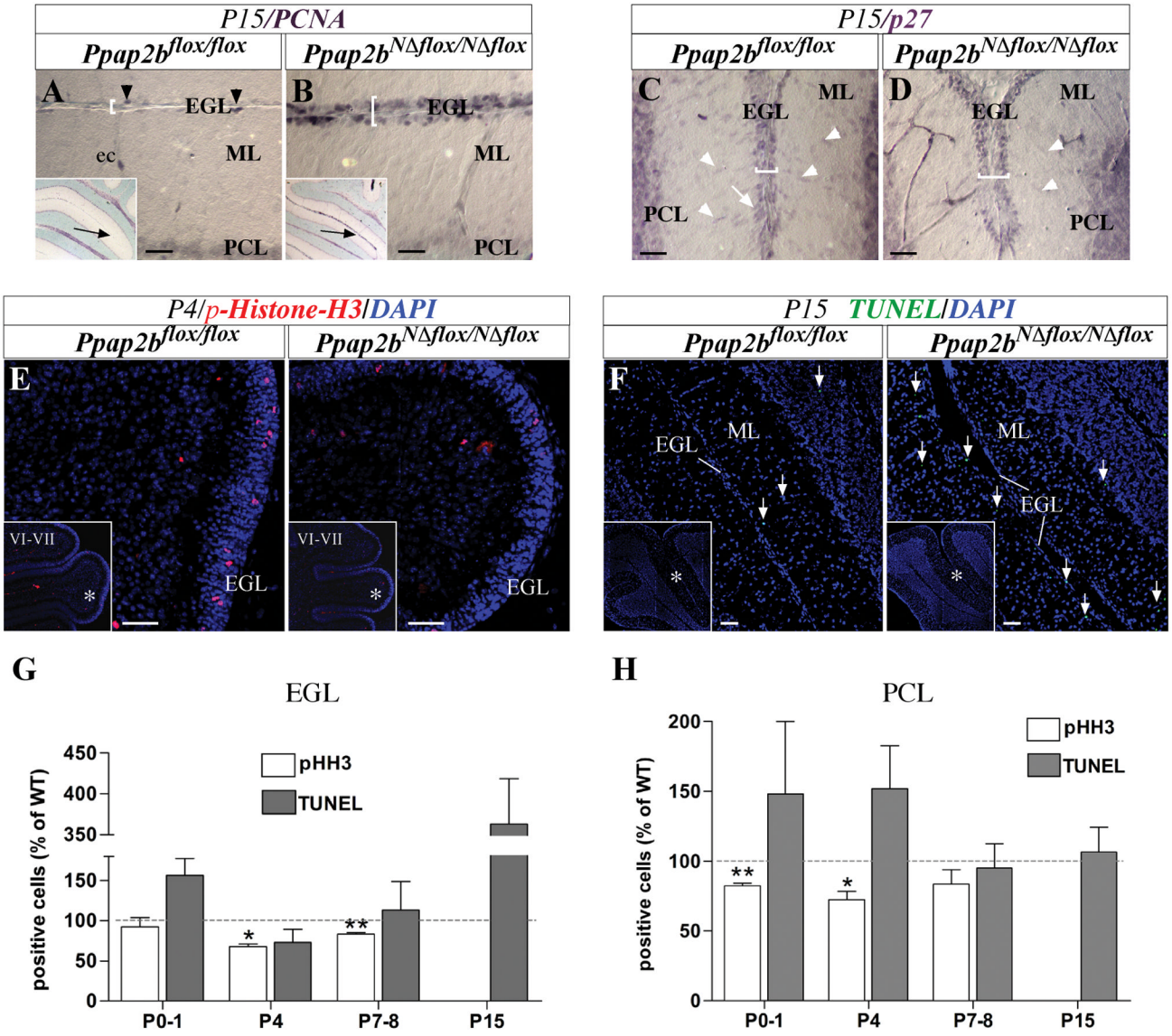

Figure 7. Developing LPP3-deficient cerebella show alterations in EGC migration, proliferation and cell death

Sagittal sections at the level of the vermis from *Ppap2b*$^{flox/flox}$ and *Ppap2b*$^{NΔflox/NΔflox}$ cerebella of the indicated stages processed for: immunoperoxidase against PCNA (A–B) or p27 (C–D), p-Histone-H3 immunofluorescence (E) or TUNEL (F). Images taken at the bottom of the primary fissure (A–B) in the area indicated by the arrow (insets) or at the intercrural fissure (C–D). Square brackets indicate the thickness of the labeled EGL. Arrowheads in (A) show PCNA-positive cells and in (C–D) migrating GC. (E) Representative image of p-Histone-H3 staining in cerebella at P4, the area showed corresponds to folia IV–V (asterisks in insets); note the decrease in proliferation in CKO. (F) At P15, TUNEL assay showed a considerable rise in cell death in the EGL and ML of CKO, the area showed corresponds to the secondary fissure area (asterisks in insets). (G–H) Analysis of p-Histone-H3 (pHH3) and TUNEL-positive cells in the EGL (G) and PCL (H) at the stages indicated. At least 3 animals/genotype/stage were evaluated, except for P15

TUNEL (n=2). Values are mean ± sem, t test *($p<0.05$) and **($p<0.01$). ec, endothelial cell. Scale bar: A–D, 30 μm; E–F, 50 μm.

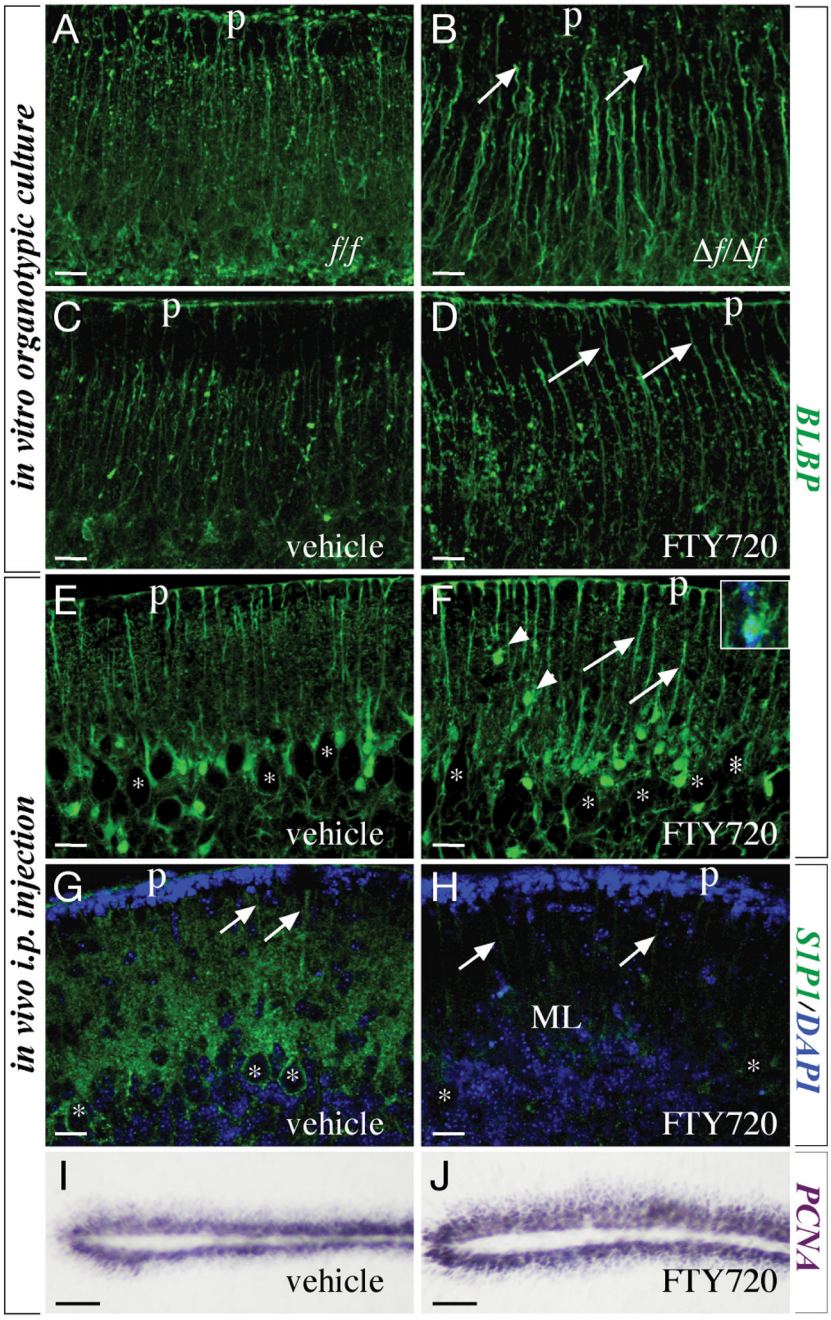

Figure 8. Treatment with FTY720 partially mimics the BG alterations seen in the neural LPP3 CKO cerebellum

BLBP detected in P7 cerebellum organotypic slice cultures from *f/f* (A) and Δ*f*/Δ*f* (B) cerebellum; note that morphology of BG is very similar to that found in non-cultured tissue, including end-feet that do not reach the pial surface (arrows), thickening of radial processes and reduction of lateral processes complexity. Organotypic culture from wildtype cerebellum sections treated with vehicle (C) or FTY720 (D); note thickening of BLBP-positive BG processes (arrows) in those treated with the drug. A slight decrease in lateral processes complexity is detected. Detection of BLBP (E–F), $S1P_1$ (G–H) or PCNA (I–J) in P14 cerebellum sections from wildtype animals treated 11 days with vehicle (E, G, I) or

FTY720 (F, H, J). (E, F) In FTY720-treated animals, thickening of BG processes (arrows in F), irregular arrangement of BG somas within the PCL and ectopic somas in the ML (arrowheads and inset in F) were found. (G, H) FTY720 treatment causes a strong, although not complete, down-regulation of $S1P_1$, since some staining was still observed in the ML and in some BG shafts (compare the staining labeled by arrows in G and H). (I, J) The thickness of PCNA-positive (dark purple) intercrural EGL in FTY720 treated animals was larger than in controls. Arrows in G indicate $S1P_1$-positive BG radial processes. Asterisks in E–H indicate Purkinje cell somas; p; pial surface. Scale bar: A–H, 20 μm; I–J, 40 μm.